



**Titre:** An electrochemical study of natural and chemically controlled  
Title: eumelanin

**Auteurs:** Ri Xu, Carmela Tania Prontera, Eduardo Di Mauro, Alessandro  
Authors: Pezzella, Francesca Soavi, & Clara Santato

**Date:** 2017

**Type:** Article de revue / Article


**Référence:** Xu, R., Prontera, C. T., Di Mauro, E., Pezzella, A., Soavi, F., & Santato, C. (2017). An  
Citation: electrochemical study of natural and chemically controlled eumelanin. APL  
Materials, 5(12), 126108 (8 pages). <https://doi.org/10.1063/1.5000161>

 **Document en libre accès dans PolyPublie**  
Open Access document in PolyPublie

**URL de PolyPublie:**  
PolyPublie URL: <https://publications.polymtl.ca/5177/>

**Version:** Version officielle de l'éditeur / Published version  
Révisé par les pairs / Refereed

**Conditions d'utilisation:**  
Terms of Use: CC BY

 **Document publié chez l'éditeur officiel**  
Document issued by the official publisher

**Titre de la revue:** APL Materials (vol. 5, no. 12)  
Journal Title:

**Maison d'édition:** AIP Publishing  
Publisher:

**URL officiel:** <https://doi.org/10.1063/1.5000161>  
Official URL:

**Mention légale:** © 2017 Author(s). All article content, except where otherwise noted, is licensed under a  
Legal notice: Creative Commons Attribution (CC BY) license  
(<http://creativecommons.org/licenses/by/4.0/>)

# An electrochemical study of natural and chemically controlled eumelanin

Cite as: APL Mater. 5, 126108 (2017); <https://doi.org/10.1063/1.5000161>

Submitted: 14 August 2017 • Accepted: 08 December 2017 • Published Online: 29 December 2017

Ri Xu, Carmela Tania Prontera, Eduardo Di Mauro, et al.



View Online



Export Citation



CrossMark

## ARTICLES YOU MAY BE INTERESTED IN

[Melanin as an active layer in biosensors](#)

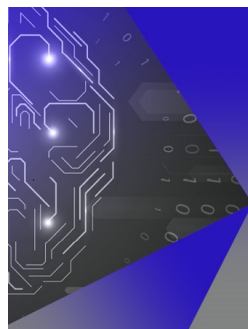
AIP Advances **4**, 037120 (2014); <https://doi.org/10.1063/1.4869638>

[On the origin of electrical conductivity in the bio-electronic material melanin](#)

Applied Physics Letters **100**, 093701 (2012); <https://doi.org/10.1063/1.3688491>

[Synthetic melanin thin films: Structural and electrical properties](#)

Journal of Applied Physics **96**, 5803 (2004); <https://doi.org/10.1063/1.1803629>



## APL Machine Learning

Machine Learning for Applied Physics  
Applied Physics for Machine Learning

**First Articles  
Now Online!**

## An electrochemical study of natural and chemically controlled eumelanin

Ri Xu,<sup>1</sup> Carmela Tania Prontera,<sup>2</sup> Eduardo Di Mauro,<sup>1</sup> Alessandro Pezzella,<sup>2,a</sup> Francesca Soavi,<sup>3,a</sup> and Clara Santato<sup>1,a</sup>

<sup>1</sup>Department of Engineering Physics, Polytechnique Montreal, C.P. 6079, Succ. Centre-ville, Montreal, Quebec H3C 3A7, Canada

<sup>2</sup>Dipartimento di Scienze Chimiche, Università di Napoli Federico II, Via Cintia 4, 80126 Napoli, Italy

<sup>3</sup>Dipartimento di Chimica “Giacomo Ciamician,” Alma Mater Studiorum—Università di Bologna, Via Selmi, 2, 40126 Bologna, Italy

(Received 14 August 2017; accepted 8 December 2017; published online 29 December 2017)

Eumelanin is the most common form of the pigment melanin in the human body, with functions including antioxidant behavior, metal chelation, and free radical scavenging. This biopigment is of interest for biologically derived batteries and supercapacitors. In this work, we characterized the voltammetric properties of chemically controlled eumelanins produced from 5,6-dihydroxyindole (DHI) and 5,6-dihydroxyindole-2-carboxylic acid (DHICA) building blocks, namely, DHI-melanin, DHICA-melanin, and natural eumelanin, extracted from the ink sac of cuttlefish, *Sepia melanin*. Eumelanin electrodes were studied for their cyclic voltammetric properties in acidic buffers including Na<sup>+</sup>, K<sup>+</sup>, NH<sub>4</sub><sup>+</sup>, and Cu<sup>2+</sup> ions. © 2017 Author(s). All article content, except where otherwise noted, is licensed under a Creative Commons Attribution (CC BY) license (<http://creativecommons.org/licenses/by/4.0/>). <https://doi.org/10.1063/1.5000161>

Eumelanin is a black-brown biopigment found in the human body (e.g., in skin, hair, and eyes), in other mammals, reptiles, amphibians, fishes, and in invertebrates, such as cuttlefish and insects.<sup>1,2</sup> Eumelanin extracted from the ink sac of cuttlefish is commonly called *Sepia melanin*.

The biological functions of eumelanin include photoprotection, metal chelation, antioxidant activity, and free radical scavenging.<sup>3</sup> Neuromelanin, a pigment made of eumelanin and pheomelanin (a yellow-red member of the melanin pigment family) present in the brain of humans and primates, is reported to be involved in neurotransmission in the *substantia nigra* of the brain.<sup>4</sup>

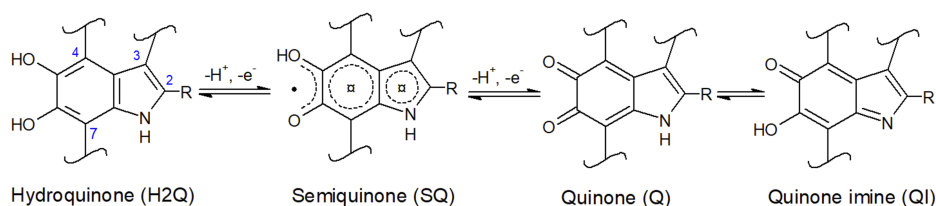
Exciting technologies based on eumelanin have been recently demonstrated, such as biologically derived batteries and flexible micro-supercapacitors for edible electronics and electroceuticals.<sup>5–7</sup>

The heterogeneous eumelanin macromolecules are constituted by the building blocks 5,6-dihydroxyindole (DHI) and 5,6-dihydroxyindole-2-carboxylic acid (DHICA). The building blocks can polymerize at different positions (indicated as 2, 3, 4, and 7 in Scheme 1). Different redox states of the building blocks, namely, hydroquinone, semiquinone, and quinone, coexist in eumelanin (Scheme 1). *Sepia melanin* is made up of DHI and DHICA building blocks and includes a wide range of cations, e.g., Mg<sup>2+</sup>, Ca<sup>2+</sup>, Cu<sup>2+</sup>, and Fe<sup>3+</sup>.<sup>1,8–10</sup>

Despite the tremendous interest of eumelanin and eumelanin derivatives, fundamental aspects of electron transfer processes in eumelanin are still largely undiscovered. Indeed, the limited solubility of eumelanin in most organic solvents has rendered challenging, through the years, the understanding of its physicochemical properties, including the electrochemical ones. Serpentine *et al.* studied the redox properties of DOPA-melanin by means of a carbon paste electrode at low potential scan rates.<sup>11</sup> In *thin-layer* conditions, the voltammogram of eumelanin at pH 5.6 revealed two main peaks in

Note: Invited for the “From Molluscs to Materials” special topic.

<sup>a</sup>Authors to whom correspondence should be addressed: [alessandro.pezzella@unina.it](mailto:alessandro.pezzella@unina.it), [francesca.soavi@unibo.it](mailto:francesca.soavi@unibo.it), and [clara.santato@polymtl.ca](mailto:clara.santato@polymtl.ca)



SCHEME 1. Molecular structures of 5,6-dihydroxyindole (DHI) and 5,6-dihydroxyindole-2-carboxylic acid (DHICA); R is -H in DHI and -COOH in DHICA. The redox forms of DHI and DHICA are indicated: hydroquinone (H2Q), semiquinone (SQ), and quinone (Q). The quinone imine (QI) form is the tautomer of Q.

oxidation, at 460 and 525 mV versus SCE (saturated calomel electrode), one of the two attributable to the oxidation of an amino group of the indole unit of eumelanin, and two peaks in reduction, at 20 and 355 mV vs. SCE. The same authors did not observe any anodic peak attributable to 5,6-dihydroxyindole, located at 50 mV vs. SCE at pH 7.4, in contrast with Young *et al.*<sup>12,13</sup> Gidianian *et al.* reported on the cyclic voltammetric polymerization of DHI building blocks, carried out between -0.35 V and 0.4 V vs Ag/AgCl, on gold disk electrodes, in phosphate buffers at pH 7.0.<sup>14</sup> More recently, Kumar *et al.*, reporting on eumelanin-based micro-supercapacitors, observed the absence of distinguishable voltammetric signatures, attributed to the convolution of several redox processes taking place at redox sites featuring different molecular environments.<sup>7</sup>

To assess the technological potential of eumelanin, it is imperative to systematically study electron transfer processes taking place at eumelanin-based electrodes. The scientific relevance of this type of study depends dramatically on the capability to control the molecular structure of the eumelanin and, considering the binding affinity of eumelanin for metal cations, on the choice of the electrolyte. Indeed, the molecular structure determines the nature of the redox sites where the electron transfer takes place. On the other hand, the electrolyte composition, and specifically the cation chemistry and its binding affinity to eumelanin, affects thermodynamic and kinetic aspects of the redox process.

In this work, we report on the cyclic voltammetric study of chemically controlled eumelanins obtained from the solid-state polymerization of DHI and DHICA building blocks, namely, DHI-melanin and DHICA-melanin. The study has been conducted in slightly acidic electrolytes, based on the well-established proton transport properties of eumelanin.<sup>7,15,16</sup> Different aqueous electrolytes were considered, including monovalent ( $\text{NH}_4^+$ ,  $\text{Na}^+$ ,  $\text{K}^+$ ) and divalent cations ( $\text{Cu}^{2+}$ ). Afterwards, the behavior of DHI-melanin and DHICA-melanin has been compared to that of *Sepia* natural eumelanin.

Chemically controlled eumelanins, i.e., DHI-melanin and DHICA-melanin, were synthesized *in situ* on carbon paper electrodes by a solid-state polymerization method already reported in the literature.<sup>17</sup> Specifically, 10 mg/ml solutions of DHI and DHICA monomers in methanol were prepared in ambient conditions. The monomer solution (5  $\mu\text{l}$ ) was drop cast on the carbon paper (Spectracarb™ 2050A, 10 mil, geometric area 0.5  $\text{cm}^2$ ). The loading of DHI-melanin or DHICA-melanin on each carbon paper electrode was ca 0.1  $\text{mg cm}^{-2}$ . After drop casting, the samples were exposed to  $\text{NH}_3$  vapors from  $\text{NH}_3(\text{aq})$  (Sigma Aldrich, 28%-30% w/v) to catalyze the reaction. The polymerization takes about 3 h for DHI and about 16 h (overnight) for DHICA. For *Sepia* melanin, we drop cast on carbon paper solutions of filtered *Sepia* melanin (Sigma Aldrich) in DMSO (Sigma Aldrich,  $\geq 99.9\%$ ). *Sepia* was indeed dissolved in DMSO, sonicated, and filtered (0.1 mm PTFE membrane with polypropylene housing, 25 mm diameter, PURADISC™), to yield suspensions of 10  $\text{mg ml}^{-1}$ , approximately (as some eumelanin aggregates may have been trapped in the filter).<sup>18,19</sup> 0.25M buffer solutions of  $\text{NH}_4\text{CH}_3\text{COO}$ ,  $\text{NaCH}_3\text{COO}$ , and  $\text{KCH}_3\text{COO}$ , pH ca 5, were prepared from  $\text{NH}_4\text{CH}_3\text{COO}$  (Caledon,  $\geq 97.0\%$ ),  $\text{NaCH}_3\text{COO}$ , and  $\text{KCH}_3\text{COO}$  (Sigma Aldrich,  $\geq 99.0\%$ ) dissolved in DI water (18.2  $\text{M}\Omega \text{ cm}$ ). 2.5 mM  $\text{Cu}(\text{CH}_3\text{COO})_2$  solution in 0.25M  $\text{NH}_4\text{CH}_3\text{COO}$  buffer was prepared using  $\text{Cu}(\text{CH}_3\text{COO})_2$  from Sigma-Aldrich (98+%). Cyclic voltammetry was performed using a Biologic VSP 300 multichannel potentiostat in a three-electrode cell, where carbon paper electrodes loaded with eumelanin were the working electrodes, a Pt mesh was the counter electrode and  $\text{Ag}/\text{AgCl}(\text{aq})$  was the reference electrode. Fresh electrodes were cycled in the potential range -0.2 V/0.2 V, -0.4 V/0.4 V, and -0.6 V/0.6 V vs.  $\text{Ag}/\text{AgCl}$ , for a total of 36 cycles (12 in each potential range), in  $\text{NH}_4\text{CH}_3\text{COO}$ ,  $\text{NaCH}_3\text{COO}$ , and  $\text{KCH}_3\text{COO}$  solutions and, for a total of 42 cycles



(14 cycles in each potential range) in the  $\text{Cu}(\text{CH}_3\text{COO})_2$ -including  $\text{NH}_4\text{CH}_3\text{COO}$  solution. The cyclic voltammograms (apart from those shown in Figs. S1–S3 of the [supplementary material](#)) correspond to the 28th cycle for  $\text{NH}_4\text{CH}_3\text{COO}$ ,  $\text{NaCH}_3\text{COO}$ , and  $\text{KCH}_3\text{COO}$  solutions and the 33rd cycle for the  $\text{Cu}(\text{CH}_3\text{COO})_2$ -including  $\text{NH}_4\text{CH}_3\text{COO}$  electrolyte. The first scan was performed towards positive values of the potential. The UV-vis spectra of the DHI and DHICA monomers in solution were obtained immediately after the monomers were dissolved in methanol (Sigma, anhydrous 99.8%) in ambient conditions, by a JASCO V-730 UV-visible spectrophotometer (Fig. S4 of the [supplementary material](#)). Scanning Electron Microscopy (SEM) was performed at an acceleration voltage of 5 kV in backscattered electron (BSE) imaging mode using a microscope (JEOL JSM7600F). For staining, the samples were exposed to an aqueous solution of uranyl acetate (2%) for different times and then rinsed with deionized water for 5 min. The SEM images included in this work correspond to 60 min of staining for DHICA-melanin and bare carbon papers, 3 min for DHI-melanin, and 10 min for Sepia melanin.

We characterized the morphological features of the eumelanins on the carbon paper by SEM. To distinguish the eumelanin from the carbon paper substrate, we stained the biopigment with uranyl acetate.<sup>7,20</sup> The bright regions observable in the SEM images after staining, mostly present at the junctions of the carbon fibers, indicate the presence of eumelanin (Fig. 1 and Fig. S5 of the [supplementary material](#)). Sepia melanin granules are expected to have a lower interfacial area with the electrode and the electrolyte, compared to DHI-melanin and DHICA-melanin.

We proceeded with the electrochemical characterization of DHI-melanin, DHICA-melanin, and Sepia melanin in different aqueous electrolytes, slightly acidic, in agreement with the well-established proton conduction properties of eumelanin.<sup>7,15,16</sup> The mobility of the protons in eumelanin makes them effective to counterbalance the injected/extracted charge thus promoting the redox processes.

In presence of monovalent cations, a number of electrochemical signatures of DHI-melanin, DHICA-melanin, and Sepia melanin, well distinguishable from those of the carbon paper (blank), were observable during the anodic and cathodic voltammetric scans. When explored within the potential interval  $-0.6/0.6$  V vs Ag/AgCl, the voltammograms of DHICA-melanin showed an oxidation shoulder located at ca 0.14 V and an oxidation peak at ca 0.31 V [Fig. 2(a)]. Reduction and oxidation peaks located at ca  $-0.06$  V could be also observed in the three electrolytes (not shown). The presence of different oxidation peaks is attributed to the heterogeneous structure of DHICA-melanin that features different quinone, hydroquinone, and semiquinone redox functionalities, located in building blocks with different inter-unit conjugation.<sup>21</sup> A broad reduction wave, presumably resulting from the overlap of broad peaks, was observable within the range 0.3 V and  $-0.5$  V vs. Ag/AgCl. The shape of the voltammograms of DHICA-melanin is the same for ammonium- and alkaline metal-based electrolytes whereas the intensities of the current are different. The shoulder at 0.14 V has the same intensity in  $\text{NH}_4^+$ - and  $\text{Na}^+$ -based electrolytes whereas the peak at 0.31 V is weaker in  $\text{NH}_4^+$ - than that in  $\text{Na}^+$ -based electrolytes. The situation is different for electrolytes containing  $\text{K}^+$ , where the voltammetric currents are lower than those in the other two electrolytes. In principle, the intensity of the voltammetric current is related to the kinetics of ion exchange at the eumelanin/electrolyte interface, strongly affected by the size of the ions. During the oxidation process, the acetate anions are expected to be inserted in the eumelanin network to balance the oxidation charge, whereas the cations included in the eumelanin matrix are expected to be released in the electrolyte. The difference in the current intensities for the different electrolytes can be only in part explained by considerations on the ion size since the electrolytes feature a common acetate anion and the hydrated cation radii have similar values (e.g., the mean metal–oxygen bond distance for hydrated sodium and potassium cations have been determined to be 2.43 and 2.81 Å, considering, respectively, six and seven coordination).<sup>22</sup> Specific interactions at different redox sites of DHICA-melanin immersed in the electrolytes are expected to contribute to determine the voltammetric currents. As an example,  $\text{NH}_4\text{CH}_3\text{COO}$  has acid-base properties expected to affect proton transfer processes associated with electron transfers and specific interactions between melanin and ammonium are well established in the literature.<sup>23</sup>

DHI-melanin shows a voltammetric signature different from that of DHICA-melanin, in all the electrolytes. Specifically, a broad oxidation wave is included between  $-0.35$  V and 0.4 V, which might result from the convolution of the peaks observed in DHICA-melanin. A broad reduction

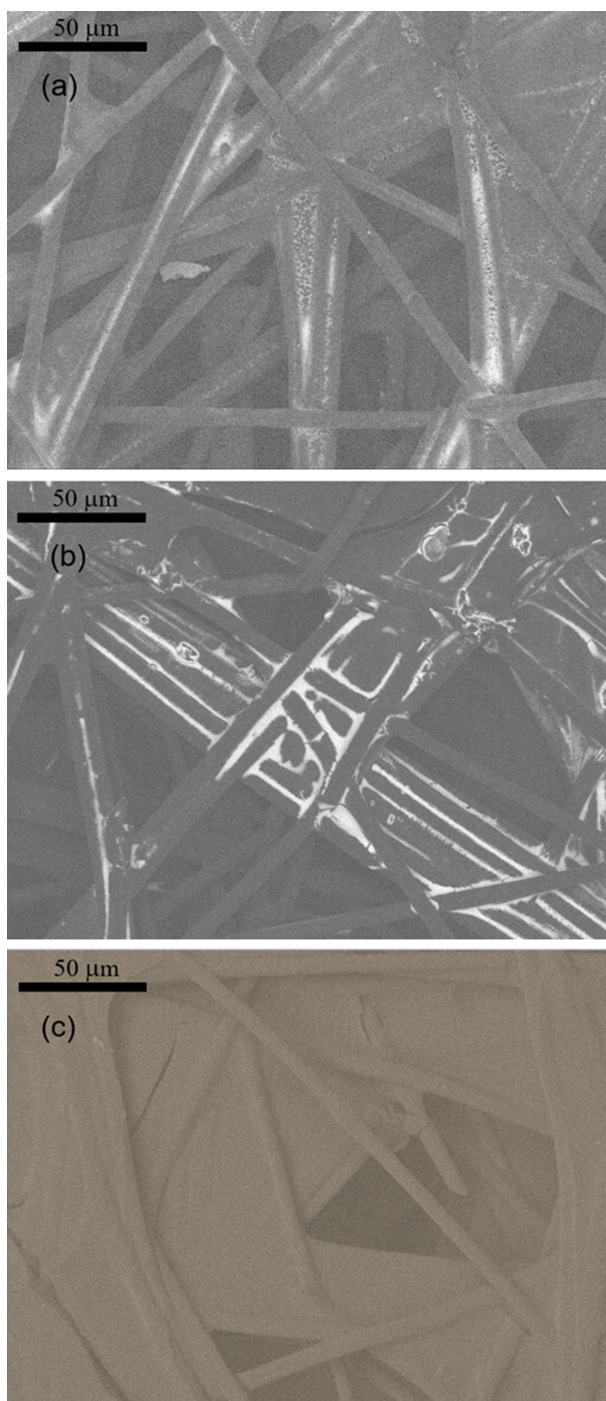


FIG. 1. SEM images (backscattering mode, acceleration voltage 5 kV) of stained (a) DHICA-melanin, (b) DHI-melanin, (c) bare carbon paper. Bar size: 50  $\mu\text{m}$ .

signature, similar to the anodic wave, is located between 0.4 V and  $-0.5$  V, as for DHICA-melanin [Fig. 2(b)]. When compared to DHICA-melanin, DHI-melanin generally shows higher ( $\sim 2$  times) voltammetric currents, likely due to the more efficient  $\pi$ - $\pi$  stacking in DHI-melanin with respect to DHICA-melanin.<sup>21</sup> The improved conjugation and corresponding electron delocalization might also explain the different shapes of the voltammograms: in DHICA-melanin, electron transfers and ion exchanges are likely more localized than those in DHI-melanin thus leading to more resolved peaks.

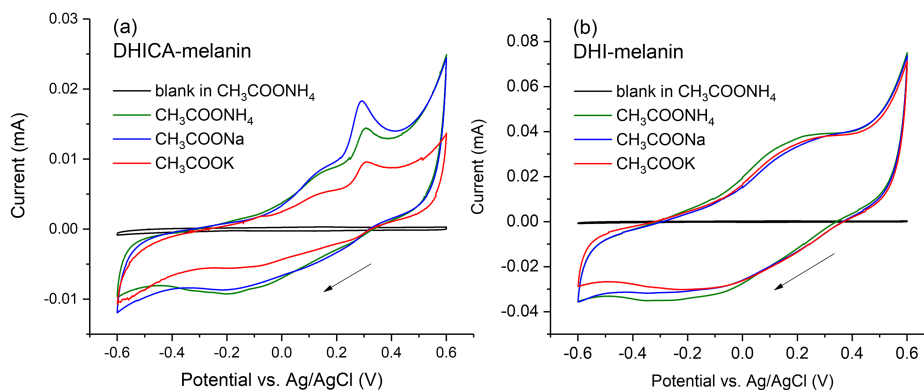


FIG. 2. Cyclic voltammograms of DHICA-melanin (a) and DHI-melanin (b) run in three aqueous electrolytes as specified in the legend. Scan rate: 5 mV/s. The electrochemical potential was cycled toward 0.6 V and then to  $-0.6$  V vs Ag/AgCl.

For both melanins, we observe a broad and irreversible peak during the initial anodic scans, for all potential ranges investigated (Fig. S1 of the [supplementary material](#)), analogously to our previous voltammetric studies conducted to advance the knowledge about mixed electronic-protonic transport in eumelanin and its exploitation for energy storage.<sup>7,16,24</sup> This broad anodic signature is attributed, at least in part, to the formation of oxidized species at the positive electrode, eventually coupling to give an increased intermolecular reticulation.<sup>18,25</sup>

With respect to DHI-melanin and DHICA-melanin, Sepia melanin in  $\text{NH}_4^+$ ,  $\text{Na}^+$ , and  $\text{K}^+$ -based electrolytes showed lower voltammetric currents (Fig. 3), possibly due to the lower interfacial area of Sepia melanin with carbon and the electrolyte, with respect to the DHI-melanin and DHICA-melanin counterparts.<sup>26</sup> Eumelanin losses during the filtration process undergone by Sepia cannot be excluded as a potential cause of decrease of the voltammetric current. Sepia melanin has oxidation and reduction signatures at ca 0.15 V as well as at ca  $-0.06$  V, analogous to DHICA-melanin.

With respect to voltammograms carried out in electrolytes including  $\text{NH}_4^+$ ,  $\text{Na}^+$ , and  $\text{K}^+$ , when  $\text{Cu}^{2+}$  is present in the electrolyte, in the form of  $\text{Cu}(\text{CH}_3\text{COO})_2$  added to our  $\text{NH}_4\text{CH}_3\text{COO}$  buffer, we observed dramatic changes in the voltammograms. Initially, with bare carbon paper electrodes (our blank), we observed an extremely broad reduction signature, attributable to the reduction of  $\text{Cu}^{2+}$  to  $\text{Cu}^+$ , located at ca  $-0.1$  V, followed by an anodic peak at 0.1 V, attributable to the re-oxidation of  $\text{Cu}^+$  to  $\text{Cu}^{2+}$  (Fig. 4). The high symmetry of the triangle-shaped oxidation peak suggests a surface redox process, involving  $\text{Cu}^+$  adsorbed on the carbon paper electrode.<sup>27</sup> With DHICA-melanin or DHI-melanin on the carbon paper, the voltammograms change: the intensity of the reduction signature is

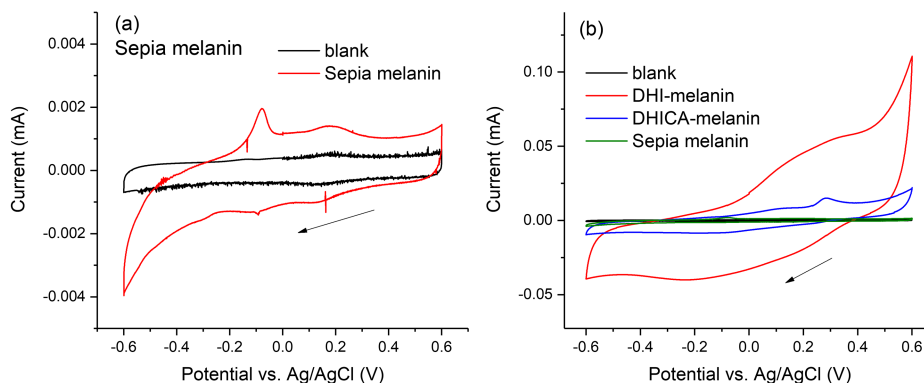


FIG. 3. Cyclic voltammograms of (a) Sepia melanin and blank electrode and (b) DHI-melanin, DHICA-melanin, Sepia melanin, and blank carbon paper electrodes in 0.25M  $\text{NaCH}_3\text{COO}_{(\text{aq})}$ . Scan rate: 5 mV/s. The potential was scanned toward 0.6 V and then backward to  $-0.6$  V vs Ag/AgCl.

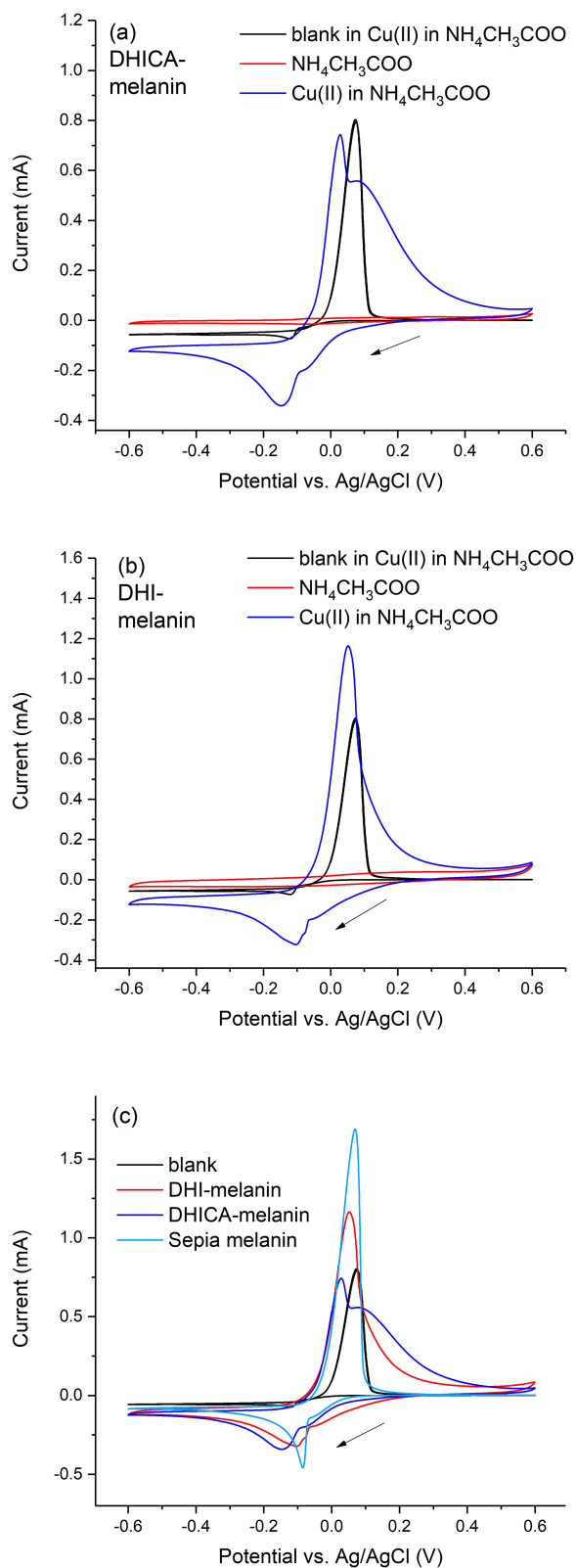


FIG. 4. Cyclic voltammograms of (a) DHI-melanin, (b) DHICA-melanin and blank carbon paper electrodes in NH<sub>4</sub>CH<sub>3</sub>COO and Cu(CH<sub>3</sub>COO)<sub>2</sub> (2.5 mM) in NH<sub>4</sub>CH<sub>3</sub>COO (0.25M) buffer solutions, (c) DHI-melanin, DHICA-melanin, Sepia melanin, and blank carbon paper electrodes in Cu(CH<sub>3</sub>COO)<sub>2</sub> (2.5 mM) in NH<sub>4</sub>CH<sub>3</sub>COO (0.25M) buffer solutions at pH 4.9 at a scan rate of 5 mV/s.

significantly higher than that for bare carbon papers [Figs. 4(a) and 4(b)]. This might be explained with a higher surface electrode concentration of  $\text{Cu}^{2+}$ , with respect to bare carbon, caused by the binding affinity of melanin for  $\text{Cu}^{2+}$ .

Concerning the oxidation, the main peak attributed to the re-oxidation of  $\text{Cu}^+$  is anticipated at lower potentials when DHI melanin and DHICA melanin are present on the carbon paper electrodes. This is explained with a weaker adsorption of the reactant ( $\text{Cu}^+$ ) at the surface of the melanin-on-carbon electrode with respect to bare carbon. Furthermore, a new broad peak (for DHICA-melanin) or shoulder (for DHI-melanin) appear at higher anodic potentials that could be assigned to the oxidation of  $\text{Cu}^+$  bound to eumelanin, formed during the cathodic scan.

Sepia melanin, known in the literature to bind  $\text{Cu}^{2+}$  at hydroxyl, carboxylic, and amine groups,<sup>1</sup> in solutions including  $\text{Cu}^{2+}$ , has sharper oxidation and reduction peaks with respect to DHI-melanin and DHICA-melanin [Fig. 4(c)]. The reduction peak is also sharpened and anticipated with respect to the carbon paper, therefore further supporting the idea of the change of the  $\text{Cu}^{2+}$  reduction to  $\text{Cu}^+$  from a solution process to a surface one, as for DHI-melanin and DHICA-melanin.<sup>27</sup> When comparing DHI-melanin, DHICA-melanin, and Sepia, we observe that the oxidation peak current is more intense with DHI-melanin and Sepia melanin and that the anodic peak (shoulder) following the main peak at 0.1 V observed with DHICA (DHI)-melanin is not observed in the voltammograms of Sepia. This suggests the availability, in DHI-melanin and DHICA-melanin, of binding sites not present in Sepia melanin, pointing to the effect of the supramolecular structure on the electron transfer between eumelanin and copper.

In conclusion, in this work, we report on the cyclic voltammetric behavior, in acidic electrolyte buffers, of chemically controlled eumelanins obtained from the solid-state polymerization of the DHI and DHICA building blocks as well as of natural eumelanin, Sepia. Eumelanin samples were fabricated on the carbon paper electrodes and studied in electrolytes including monovalent ( $\text{NH}_4^+$ ,  $\text{Na}^+$ ,  $\text{K}^+$ ) and divalent ( $\text{Cu}^{2+}$ ) cations. With respect to DHI, which shows in  $\text{NH}_4^+$ ,  $\text{Na}^+$ , and  $\text{K}^+$ -including solutions broad oxidation and reduction signatures, DHICA-melanin shows a well distinguishable oxidation signature, observable at 0.31 V. Both the voltammograms of DHICA-melanin and Sepia melanin display the redox features at  $-0.06$  V and 0.15 V. All the eumelanin samples immersed in ammonium acetate buffers including  $\text{Cu}^{2+}$  have a strong oxidation peak at 0.1 V and reduction features included between  $-0.05$  V and  $-0.09$  V (shoulder) and  $-0.09$  V and  $-0.14$  V (peak). DHI-melanin and DHICA-melanin have an additional oxidation feature at higher anodic potentials attributable to the oxidation of  $\text{Cu}^+$  bound to eumelanin, with respect to Sepia. The work is in progress to extend the present studies to other cations of biological interest, such as  $\text{Fe}^{2+}/\text{Fe}^{3+}$ , to better understand the biological function of eumelanin in living organism. Considering the optical properties of eumelanin, our work contributes to advance the development of biologically derived organic solar batteries, integrating the solar conversion and the energy storage functions.

See [supplementary material](#) for stability of the cyclic voltammograms and effect of the scan rate, SEM of bare carbon collectors, and UV-Vis spectra.

The Authors are grateful to Y. Drolet (Polytechnique Montréal) and D. Gingras (Université de Montréal) for technical support. C.S. acknowledges financial support from NSERC (DG) and MESI. A.P. acknowledges financial support from MC-IRSES-612538 (POLYMED). F.S. and C.S. acknowledge the Executive Bilateral Program Italy-Quebec 2017-2019.

<sup>1</sup> E. Di Mauro, R. Xu, G. Soliveri, and C. Santato, *MRS Commun.* **7**, 141 (2017).

<sup>2</sup> G. Prota, *Melanins and Melanogenesis* (Academic Press, San Diego, 1992).

<sup>3</sup> M. D'Ischia, K. Wakamatsu, F. Cicoira, E. Di Mauro, J. C. Garcia-Borron, S. Commo, I. Galván, G. Ghanem, K. Kenzo, P. Meredith, A. Pezzella, C. Santato, T. Sarna, J. D. Simon, L. Zecca, F. A. Zucca, A. Napolitano, and S. Ito, *Pigm. Cell Melanoma Res.* **28**, 520 (2015).

<sup>4</sup> P. Meredith, K. Tandy, and A. Mostert, in *Organic Electronics: Emerging Concepts and Technologies*, edited by C. Santato and F. Cicoira (Wiley, 2013), pp. 91–111.

<sup>5</sup> Y. J. Kim, W. Wu, S. E. Chun, J. F. Whitacre, and C. J. Bettinger, *Adv. Mater.* **26**, 6572 (2014).

<sup>6</sup> Y. J. Kim, W. Wu, S. E. Chun, J. F. Whitacre, and C. J. Bettinger, *Proc. Natl. Acad. Sci. U. S. A.* **110**, 20912 (2013).

<sup>7</sup> P. Kumar, E. Di Mauro, S. Zhang, A. Pezzella, F. Soavi, C. Santato, and F. Cicoira, *J. Mater. Chem. C* **4**, 9516 (2016).

<sup>8</sup> B. Larsson and H. Tjälve, *Acta Physiol. Scand.* **104**, 479 (1978).

<sup>9</sup> L. Hong and J. D. Simon, *J. Phys. Chem. B* **111**, 7938 (2007).

- <sup>10</sup> B. Szpoganicz, S. Gidanian, P. Kong, and P. Farmer, *J. Inorg. Biochem.* **89**, 45 (2002).
- <sup>11</sup> C. Serpentine, C. Gauchet, D. De Montauzon, M. Comtat, J. Ginestar, and N. Paillous, *Electrochim. Acta* **45**, 1663 (2000).
- <sup>12</sup> T. E. Young, J. R. Griswold, and M. H. Hulbert, *J. Org. Chem.* **39**, 1980 (1974).
- <sup>13</sup> T. E. Young, B. W. Babbitt, and L. A. Wolfe, *J. Org. Chem.* **45**, 2899 (1980).
- <sup>14</sup> S. Gidanian and P. J. Farmer, *J. Inorg. Biochem.* **89**, 54 (2002).
- <sup>15</sup> A. B. Mostert, B. J. Powell, F. L. Pratt, G. R. Hanson, T. Sarna, I. R. Gentle, and P. Meredith, *Proc. Natl. Acad. Sci. U. S. A.* **109**, 8943 (2012).
- <sup>16</sup> J. Wünsche, Y. Deng, P. Kumar, E. Di Mauro, E. Josberger, J. Sayago, A. Pezzella, F. Soavi, F. Cicoira, M. Rolandi, and C. Santato, *Chem. Mater.* **27**, 436 (2015).
- <sup>17</sup> A. Pezzella, M. Barra, A. Musto, A. Navarra, M. Alfè, P. Manini, S. Parisi, A. Cassinese, V. Criscuolo, and M. D'Ischia, *Mater. Horiz.* **2**, 212 (2015).
- <sup>18</sup> A. Pezzella, M. D'Ischia, A. Napolitano, A. Palumbo, and G. Prota, *Tetrahedron* **53**, 8281 (1997).
- <sup>19</sup> Y. Liu and J. D. Simon, *Pigment Cell Res.* **16**, 72 (2003).
- <sup>20</sup> T. Sakaguchi and A. Nakajima, *J. Chem. Technol. Biotechnol.* **40**, 133 (2007).
- <sup>21</sup> L. Panzella, G. Gentile, G. D'Errico, N. F. Della Vecchia, M. E. Errico, A. Napolitano, C. Carfagna, and M. D'Ischia, *Angew. Chem., Int. Ed.* **52**, 12684 (2013).
- <sup>22</sup> J. Mähler and I. Persson, *Inorg. Chem.* **51**, 425 (2012).
- <sup>23</sup> P. Prem, K. Dube, S. Madison, and J. Bartolone, *J. Cosmet. Sci.* **54**(4), 395 (2003).
- <sup>24</sup> L. G. S. Albano, E. Di Mauro, P. Kumar, F. Cicoira, C. F. O. Graeff, and C. Santato, *Polym. Int.* **65**, 1315 (2016).
- <sup>25</sup> A. Napolitano and A. Pezzella, *Tetrahedron* **52**, 8775 (1996).
- <sup>26</sup> E. Di Mauro, O. Carpentier, S. I. Yáñez Sánchez, N. Ignoumba Ignoumba, M. Lalancette-Jean, J. Lefebvre, S. Zhang, C. F. O. Graeff, F. Cicoira, and C. Santato, *J. Mater. Chem. C* **4**, 9544 (2016).
- <sup>27</sup> A. J. Bard and L. R. Faulkner, *Electrochemical Methods: Fundamentals and Applications*, 2nd ed. (Wiley, 2000).